Forest Ecology and Management 419–420 (2018) 10–16

Contents lists available at ScienceDirect

Forest Ecology and Management

journal homepage: www.elsevier.com/locate/foreco

New design of external heat-ratio method for measuring low and reverse rates of sap flow in thin stems

Sheng Wang[a,b], Jun Fan[a,c,*], Jiamin Ge[c], Qiuming Wang[c], Chenxu Yong[c], Wei You[a,b]

[a] State Key Laboratory of Soil Erosion and Dryland Farming on the Loess Plateau, Institute of Soil and Water Conservation, Chinese Academy of Sciences and Ministry of Water Resources, No. 26 Xinong Road, Yangling, Shaanxi Province 712100, China

[b] University of Chinese Academy of Sciences, No. 19 (A) Yuquan Road, Shijingshan District, Beijing 100049, China

[c] College of Natural Resources and Environment, Northwest A&F University, No. 3 Taicheng Road, Yangling, Shaanxi Province 712100, China

ARTICLE INFO

Keywords:
Sap-flux density
Heat-pulse method
External heat-ratio (EHR) technique
Small stems
Gauge spacings

ABSTRACT

Sap-flow techniques had limited application to thin-stemmed woody and herbaceous species and to diverse functional plant organs until the recent development of the external heat-ratio (EHR) method. Existing EHR techniques using miniature gauge configurations, however, are limited to thin stems with diameters of 2–5 mm. This study introduces a new design of an EHR gauge adapted to thin stems with diameters up to 15 mm and sap-flux densities $< 50\ cm\ h^{-1}$. The gauge was calibrated on cut stems of the shrubs *Caragana korshinskii* and *Salix psammophila*, with the measured heat-pulse velocity (V_h) compared to gravimetric measurements of sap-flux density (V_s) under controlled conditions. A validation test was also carried out by comparing EHR method with the stem heat-balance (SHB) method through in situ and long-term monitoring of V_s on standing stems of *C. korshinskii*. V_h in the tested cut stems of both species was linearly correlated with V_s up to approximately $50\ cm\ h^{-1}$ (R^2 up to 0.96, $P < 0.001$) in a range of stem diameters of 4.1–15.6 mm. An empirical multiplier for converting the measured V_h to V_s, however, varied between the two species, 2.02 and 1.15 for *C. korshinskii* and *S. psammophila*, respectively. The EHR technique sensitively captured the diurnal dynamics of V_s in field tests, within a range from zero to nearly $30\ cm\ h^{-1}$ on *C. korshinskii* stems, and hourly V_s was linearly correlated with the reference evapotranspiration ($R^2 = 0.70$, $P < 0.001$) over 26 successive days without drought stress. The tested SHB method, however, poorly detected the sap-flux density, especially at low densities. The gauges for the EHR method were easy to build and capable of accurate estimating bidirectional sap flow, especially at low densities. This technique, with variable EHR gauge configurations, has broader applications than SHB methods for understanding plant-water relations in understories, shrubs and ecosystems dominated by herbage.

1. Introduction

Quantifying the rate of sap flow in woody and herbaceous plants contributes to a better understanding of whole-plant water uses and plant-water relations (David et al., 2013; Steppe et al., 2015). Heat-based techniques for measuring sap flow have abundant applications in disciplines such as plant physiology, hydrology and agronomy (Rosner et al., 2018). The investigation of water transfer *in vivo* has identified the strategic “hydraulic lift” or “hydraulic redistribution” in plant-root systems in response to drought stress, especially in arid and semi-arid areas (Burgess et al., 1998; Nadezhdina et al., 2015). Continuous monitoring of whole-plant transpiration provides an alternative for studying stomatal physiological responses to transient environmental conditions (Hernandez-Santana et al., 2016; Nakano et al., 2015). Understanding the regulation of plant-water use in orchards or other crops contributes to the development of scientific and efficient irrigation schedules and management (Eastham and Gray, 1998; Fernandez et al., 2011).

Heat has been widely used as a tracer for determining the rate of sap flow in plants, and a wide range of heat-based techniques have been developed. They determine sap flow mainly by measuring the effect of mobile sap on the heat balance (Smith and Allen, 1996; Trcala and Cermak, 2016) or thermal dissipation (Lu et al., 2004) of a steadily heated portion of a stem or on the propagation of a discrete heat pulse released into a stem (Burgess et al., 2001; Marshall, 1958). The heat-based techniques can be either invasive or noninvasive to stems. Invasive techniques generally use needle-based probes, which can obstruct pathways of sap flow and damage hydroactive tissues. The effects

* Corresponding author at: Institute of Soil and Water Conservation, Chinese Academy of Sciences and Ministry of Water Resources, No. 26 Xinong Road, Yangling, Shaanxi Province 712100, China.
E-mail address: fanjun@ms.iswc.ac.cn (J. Fan).

https://doi.org/10.1016/j.foreco.2018.03.020
Received 21 November 2017; Received in revised form 11 March 2018; Accepted 13 March 2018

of these wounds can lead to underestimates of sap flow, especially for techniques based on heat pulses (Burgess et al., 2001; Green et al., 2009) and likely other methods (Steppe et al., 2015). This problem is usually solvable by applying numerical correction models for heat-pulse methods and may even become negligible for thermal-dissipation methods for plants with large stems (Lu et al., 2004). The insertion of probe needles into thin stems, however, risks breaking the fragile plant tissues; large wounds to thin stems will obstruct water and mass transfer, change plant physiological status and subsequently affect the rate of sap flow *in vivo*, thus leading to meaningless or atypical sap-flow measurements. Most invasive techniques adopting needle-based probes are therefore likely less suitable for stems typically < 10 mm in diameter (Clearwater et al., 2009). External sap-flow gauges are non-invasive and preferable for thin stems, but current stem heat-balance (SHB) methods are intrinsically limited by the poor detection of low rates of sap flow, because they require many empirical settings to acquire heat-balance terms (Grime and Sinclair, 1999).

The recently developed external heat-ratio (EHR) technique provides a promising approach to the non-destructive and accurate determination of bidirectional sap flow in thin stems. Clearwater et al. (2009) developed a miniature, external gauge that could be tightly mounted onto the surface of plant organs and stems. It determines sap flow using the heat-ratio equation established by Marshall (1958) from records of increases in temperature at equal spacings of 5 mm above and below a small heating chip after the release of a heat pulse. Miniature gauges using similar configurations were then applied to diverse functional types in a shrubland (Skelton et al., 2013) and to the water dynamics of flowering plants (Roddy and Dawson, 2012). The gauges had good applicability for stems with diameters up to 5 mm and densities of sap flux between 0.36 and 50 cm h^{-1}, but the gauges have rarely been applied to thin stems with larger diameters. Stems can be larger in regions dominated by small-stemmed shrubs, herbaceous plants and co-existing species of diverse morphologies. For example, stem diameters of *Caragana korshinskii* and *Salix psammophila*, the two dominant shrubs in an area referred to as the “water-wind erosion crisscross region” on the Loess Plateau in China, are most frequently ~10 mm. Extending the application of the EHR technique to larger stems for detecting sap flow is thus of great interest.

The configurations of current miniature external gauges, however, have several issues of potential concern. First, most gauges have narrow spacings of 5 mm from the center of the heating chip to the bilateral temperature sensors. The heat source on the external surface of the stem is assumed to release heat on a plane normal to the axial direction. The heat will clearly also travel both above and below this plane within non-hydroactive bark tissues and become dispersed as it reaches into the hydroactive xylem. The heat-ratio signals from the mobile sap will thus attenuate, especially in larger stems with thicker bark. The very narrow spacings will also amplify the effects of sensor misalignment and nonhomogeneity in contiguous bark. Second, the heater and temperature sensors of the gauges are housed in a rectangular block of nonconductive silicone/cork, which shields ambient heat only on one side of the stem at the mount location. The measured signals of temperature rise will thus contain intensive noise from shifts in ambient heat from poor insulation, especially under field conditions, probably accounting for the unexpected fluctuations common in measurements of sap-flux density (Clearwater et al., 2009; Skelton et al., 2013). Third, the heater elements use a narrow, rectangular chip resistor that can more easily break off than a circular chip, because the rectangular chip is unevenly loaded when it is pressed transversely onto cylindrical stems. This study developed a newly designed EHR gauge to fit thin stems with larger diameters, primarily by increasing the spacings between the heater and temperature sensors to 10 mm, replacing the rectangular silicone/cork with a flexible adiabatic film that can be tightly wrapped around the stem, using a circular heating chip and increasing the heating strength. The amplitude of temperature rises is lower for larger spacings (Marshall, 1958), so more heat is required to generate adequate signals of temperature rise for sensitive recordings under limited thermometric resolution in measuring systems. We tested the newly designed EHR gauge by both gravimetric measurements of flow in cut stems of *C. korshinskii* and *S. psammophila* with diameters ranging from 5 to 15 mm under controlled conditions and long-term estimation of sap-flux density of *C. korshinskii* stems in the field, compared to an SHB method.

2. Materials and methods

2.1. Design of the external heat-ratio gauge

The main body of the EHR gauge consisted of a small heater and two temperature sensors at equal spacings of 10 mm from the center of the heater, arrayed in line and adhered to the inner surface of a flexible adiabatic film. The temperature sensors were constructed using fine-gauge (30 AWG) copper-constantan thermocouple junctions (OMEGA Engineering Inc., Stamford, USA). Both of the metallically dissimilar conductors of the thermocouple were uncoupled at one end and pierced separately through the adiabatic film from the exterior surface to the inner face and joined together with tin-lead solder, keeping the inner section of the junctions normal to the axis of the stem. The adiabatic film was a spooled flexible porous polyethene sheet with tinfoil on the exterior surface. A small circular metallic-ceramic heating chip (4 mm in diameter, 1.2 mm thick, 12 Ω of resistance; Fangzhou Electric Heating Appliances Inc., Beijing, China) was attached to the center of the inner surface of the adiabatic film and acted as the heater (Fig. 1). Individual thermocouple wires and the heater electrical pins were connected to a split conductor of a specific length for connecting the EHR gauge to a data logger.

The EHR gauge is installed on a stem in an appropriately smooth area away from knots, keeping the mount location clean and dry. The gauge is tightly wrapped around the stem to ensure robust thermal contact between the thermocouple junctions, heating chip and the stem surface. A waterproof and adiabatic cover should be firmly strapped around the outside of the gauge and stem to minimize the effects of ambient heat shifts and weather.

2.2. Theory of sap flow

Clearwater et al. (2009) developed the framework of EHR gauges, which has been widely adopted. This method uses the heat-ratio

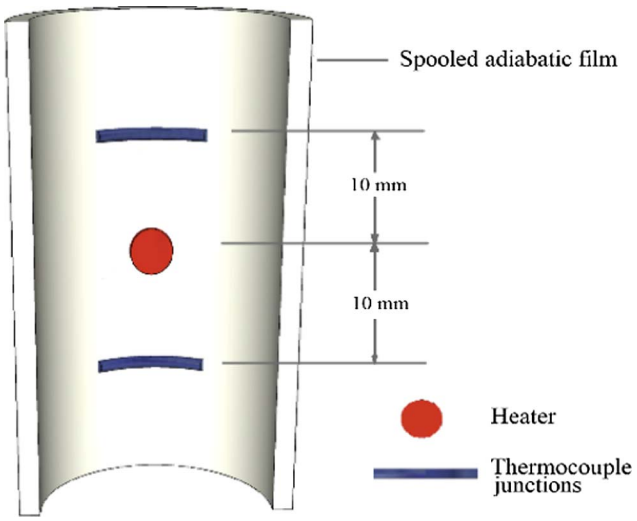

Fig. 1. Schematic diagram of the external heat-ratio gauge. The heater is a small metallic-ceramic heating chip, the temperature sensors are composed of fine-gauge (30 AWG) copper-constantan thermocouple junctions and the adiabatic film is a flexible porous polyethene sheet with tinfoil on the exterior surface.

Table 1
Properties of the cut-stem sections used for gravimetric gauge calibration, and a summary of the calibration results. Properties were stem diameter, bark thickness at the gauge mounting position, dry-wood bulk density and voulmetric water content.

Species	No.	Stem diameter mm	Bark thickness mm	Stem bulk density, ρ_b g cm^{-3}	Volumetric water content, θ cm^3 cm^{-3}	Gauge spacings, x mm	Thermal diffusivity, κ 10^{-3} cm^2 s^{-1}	m_{stem}	m_{bark}	m_{sap}
Caragana korshinskii	1	4.08	0.80	0.795 ± 0.015a	0.504 ± 0.008b	10.0	2.37 ± 0.02b	0.78	2.59	2.02
	2	4.80	0.82							
	3	7.56	0.94							
	4	10.20	0.98							
	5	13.13	1.04							
	6	13.44	1.04							
Salix psammophila	7	5.81	0.42	0.639 ± 0.012b	0.573 ± 0.010a	10.0	2.54 ± 0.02a	0.67	1.70	1.15
	8	9.73	0.64							
	9	15.60	0.72							
	10	7.15	0.56							

Note: m_{stem} is the multiplier in Eq. (6), calculated as $\rho_b(c_w + \theta c_s)/\rho_s c_s$, linearly correlating sap-flux density (V_s) with corrected heat-pulse velocity (V_c). m_{sap} is the slope of the relationship between V_s and measured heat-pulse velocity (V_h) in Eq. (8). m_{bark} is a multiplier accounting for the effects of non-hydroactive bark in Eq. (5), identical to m_{sap}/m_{stem}. Different lowercase letters indicate significant differences at $P < 0.01$. Means ± standard deviations where applicable.

equation (Marshall, 1958) to detect sap flow, following the needle-based heat-ratio method (Burgess et al., 2001). The ratio of the downstream temperature rise, ν_d, to the upstream temperature rise, ν_u, provides an accurate estimate of the velocity of the heat pulse after its release:

$$V_h = \frac{\kappa}{x}\ln(\nu_d/\nu_u)\cdot 3600, \quad (1)$$

where κ is thermal diffusivity in the axial direction (cm^2 s^{-1}), x is the spacing (cm) from the heater to the bilateral thermometric elements and V_h is a weighted average of the heat-pulse velocity of the sap and stationary stem matrix (cm h^{-1}). Thermal diffusivity can be determined by recording the temperature rise at one temperature sensor following a heat pulse, under zero-flow conditions:

$$\kappa = \frac{x^2}{4t_m}, \quad (2)$$

where t_m is the amount of time it takes a temperature sensor to reach a maximum temperature rise. Correction for sensor misalignment is also conducted under zero-flow conditions (Burgess et al., 2001):

$$x_d = \sqrt{x_u^2 - 4\kappa t\ln(\nu_d/\nu_u)|_{zero-flow}}, \quad (3)$$

where x_d and x_u are the spacings (cm) of the downstream and upstream temperature sensors from the heater, respectively, and t is the time after the release of the heat pulse (s). When x_u is assumed to be correctly spaced, x_d denotes an incorrectly spaced sensor and can be calculated from Eq. (3). Corrected V_h can be calculated as:

$$V_h = \frac{4\kappa t\ln(\nu_d/\nu_u) - x_u^2 + x_d^2}{2t(x_d - x_u)} \quad (4)$$

V_h is expected to be lower than predicted by heat-pulse theory alone due to the effects of non-hydroactive components within the system (e.g. bark and gauge materials). Clearwater et al. (2009) corrected for this effect by applying:

$$V_c = V_h\, m_{bark}, \quad (5)$$

where V_c is the corrected heat pulse velocity (cm h^{-1}), m_{bark} is an empirical multiplier accounting for this effect. Sap-flux density (V_s, cm h^{-1}) can then be described on area basis by measuring the proportions of sap and wood and by accounting for stem bulk densities and specific-heat capacities (Barrett et al., 1995):

$$V_s = \frac{V_c\rho_b(c_w + \theta c_s)}{\rho_s c_s}, \quad (6)$$

which can be written as:

$$V_s = V_c\, m_{stem}, \quad (7)$$

where ρ_b is sapwood bulk density (g cm^{-3}, dry weight/fresh volume), c_s and c_w are the specific-heat capacities of sap and wood (J kg^{-1} °C^{-1}), respectively, θ is the volumetric water content of the sapwood (cm^3 cm^{-3}) and ρ_s is the density of the sap (g cm^{-3}). Only a portion of the cross section of a stem, however, is hydroactive xylem, so correctly measuring these properties is difficult for thin stems. Here we identify a multiplier, m_{stem}, to quantify the effects of the stem properties, identical to the expression $\rho_b(c_w + \theta c_s)/\rho_s c_s$ in Eq. (6). Measured V_h was transformed into V_s for calibration and practical purposes using an empirical multiplier, m_{sap}:

$$V_s = m_{sap}\, V_h, \quad (8)$$

where m_{sap} is a coefficient that incorporates some of the effects, m_{bark} and m_{stem}, described in Eqs. (5) and (7), respectively. Sap-flow rate (J, g h^{-1}) was calculated as the product of V_s and the total cross-sectional area of a stem at the point of gauge attachment, instead of the effective "sapwood" area used by Cohen et al. (1981) and Clearwater et al. (2009). V_s is sensitive to errors in the estimation of cross-sectional areas, because determining the effective 'sapwood' area in thin stems is difficult. The transfer of heat between hydroactive and non-hydroactive tissues within a small stem is rapid, so the inclusion of total cross-sectional area may also help to reduce variability in m_{sap}.

2.3. Gauge calibration using gravimetric measurements of flow

The EHR gauges were calibrated on sections of cut stems of two shrub species, *C. korshinskii* and *S. psammophila*, using gravimetric measurements of sap flow. These two species are common local shrubs on the Loess Plateau. They have been widely planted for facilitating the conservation of soil and water, improving the fragile ecosystem and restoring vegetation. *C. korshinskii* is classified as a ring-porous species, and *S. psammophila* a diffusive-porous species. The basic properties of selected cut stems, diameter, bark thickness, bulk density and volumetric water content, are listed in Table 1.

The EHR gauges were calibrated under controlled water-flow conditions using cut-stem sections connected to a supply of purified, pressurized water. The system of gravimetric measurement of the imposed flow is shown in Fig. 2. The density of the water flux was regulated by adjusting the water head, h (m), between a Mariotte's bottle and the cut-stem section. The bottle stood upright on a smooth slope, and we moved its position along the slope to alter the elevation of the atmosphere-water interface. The maximum h was 15 m (corresponding to a water pressure of 150 kPa). An EHR gauge was mounted on each cut-stem section. The stem ends were recut under water, and one end was then inserted into the compression fitting and connected to the

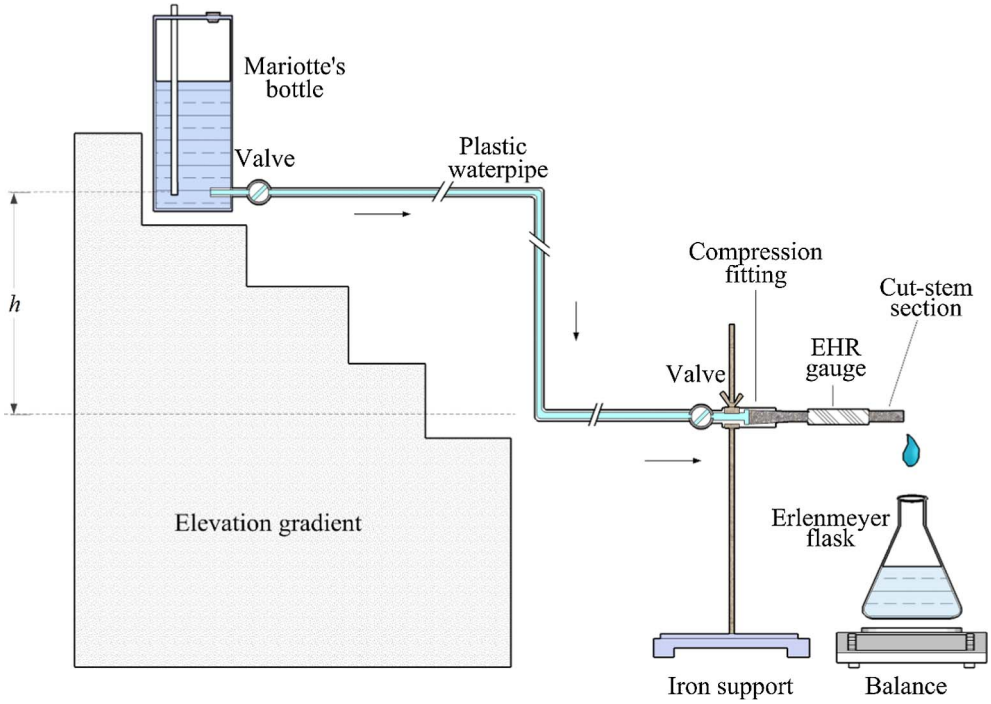

Fig. 2. Schematic diagram of the apparatus and attachments for calibrating the external heat-ratio (EHR) gauge using gravimetric measurements of flow. Arrows indicate the direction of water flow in the gravimetric measurement system. *h* denotes the controlled water head (m) for generating pressure and water flow in the cut-stem section.

measuring system. The system was inspected for functionality, the water head was set and maintained at controlled increments and the outlet water was collected at the other end with an Erlenmeyer flask and weighed using an electronic balance. V_s was then calculated from the mass of water flow, stem cross-sectional area and duration of water flow. The signals from the EHR gauges were simultaneously recorded. Gravimetric flow was measured every 30 min under conditions of stabilized flow, and measurement by the EHR gauge was triggered in the mid of each gravimetric low measurement. The signals were logged by a programmed CR3000 datalogger (Campbell Scientific Inc., Logan, USA).

2.4. Field tests

Field tests were performed in a *C. korshinskii* field in the Liudaogou catchment (38.78°N, 110.35°E; 1200 m a.s.l.), Shenmu, Shaanxi, China. The catchment is within the area of the Loess Plateau referred to as the "water-wind erosion crisscross region". Mean annual precipitation is 440 mm. The *C. korshinskii* was planted 15 years ago. The main soil type was a loessial soil consisting of 52.5% sand (> 0.05 mm), 35.8% silt (0.002–0.05 mm) and 11.7% clay (< 0.002 mm).

Three standing *C. korshinskii* stems were selected to test the EHR gauges in the field, and V_s was determined by transformation from mass sap-flow rate using SHB gauges per unit cross-sectional area for comparison. Stem diameters at the EHR gauge mounting position were 9.12, 8.76 and 9.70 mm. One EHR gauge was mounted on each stem, following the above instructions. The heater was powered at 4.5 V and 1.6 W, generating a heat pulse of 5 s. These gauges were connected to a programmed CR3000 datalogger (Campbell Scientific Inc., Logan, USA) to measure the heat pulses and estimate V_s every 30 min.

One SHB gauge (Model SGB 9, Dynamax Inc., Houston, USA) was also mounted 15 cm above the EHR gauge installation position to each of the three tested stems, following the manufacturer's instructions (Dynamax Inc., 2015). Average gauge signals were recorded at 30 min intervals with a CR1000 datalogger (Campbell Scientific Inc., Logan, USA). Sap-flow rate can be calculated as the residual of the energy balance, assuming steady-state conditions (i.e. no changes in stem heat storage) (Sakuratani, 1981, 1984; Baker and Van Bavel, 1987).

Reference evapotranspiration (ET_0) is a variable representing the potential evapotranspiration of a reference crop, depending on meteorological conditions. Rates of actual transpiration of specific plants or fields without drought stress are usually proportional to ET_0. *C. korshinskii* is highly tolerant to drought stress and consumes water from soil deeper than 6 m in our study field (Fan et al., 2016). Hourly ET_0 ($mm\,h^{-1}$) was calculated by the ASCE Penman-Monteith equation (Walter et al., 2000) using Ref-ET version 3.1 (www.kimberly.uidaho.edu), with the standard short grass chosen as the reference crop. Required meteorological data included hourly net radiation ($MJ\,m^{-2}\,h^{-1}$), mean air temperature (°C), relative humidity (%) at a height of 1.5 m, wind speed ($m\,s^{-1}$) at 2.0 m and soil heat flux ($MJ\,m^{-2}\,h^{-1}$) and were collected using an automatic meteorological station in this field.

2.5. Data analysis

Little attention has been given to the impact of temporal gradients in ambient temperature on methods based on heat pulses. These effects can generate errors ≥40% (Vandegehuchte et al., 2014). These errors can be easily prevented by including a temperature correction when analyzing the data and by calculating the rate of change of the natural temperature based on the temperatures measured before application of the heat pulse. Temperature correction followed Vandegehuchte et al. (2014). A one-way analysis of variance (ANOVA) was used to test for significant differences at $P < 0.01$ in bark thickness, stem bulk density and stem volumetric water content between the two shrub species to account for the differences in calibration coefficients for the EHR gauges. A linear regression analysis was performed using least squares to calibrate the EHR gauges by linearly correlating V_s with V_h under controlled conditions and to obtain the correlation between V_s and ET_0 in the field tests. The statistical analyses were performed with PASW statistics 18 (SPSS Inc., Chicago, USA).

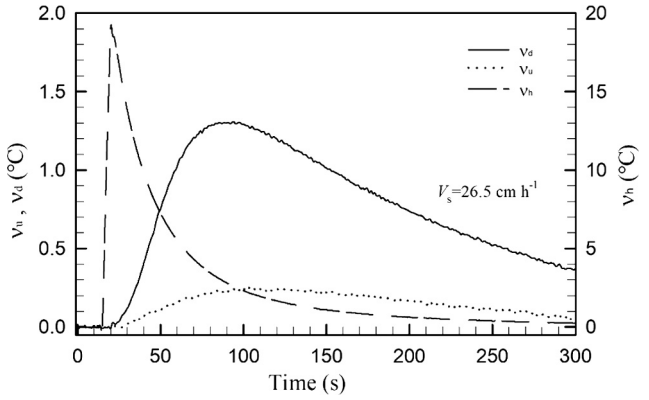

Fig. 3. Dynamics of sap-flux density (V_s) and a temperature rise (°C) over time at the heater (v_h) and the downstream (v_d) and upstream (v_u) temperature sensors of the external heat-ratio gauge during a measurement.

3. Results

3.1. Gauge calibration

The EHR gauge released a heat pulse with a period of 5 s, and the maximum temperature rise at the heater was 18.08 ± 1.40 °C. The temperatures at the upstream and downstream sensors rose rapidly after injection of the heat pulse, followed by a slow decrease to ambient temperature. The maximum temperature rise at the upstream and downstream sensors were 0.2–0.6 and 0.6–1.6 °C, respectively. Fig. 3 shows the temperature rise in response to the release of heat pulses. The difference in the temperature rise at the bilateral temperature sensors were due to heat convection by sap flow. The natural logarithm of the ratio of the temperature rise between downstream and upstream, $\ln(v_d/v_u)$, were relatively steady during each measurement, especially after 60 s, and were closely correlated with V_s. Noise from imperfect adiabatic shielding and sudden shifts in ambient temperature, however, would distort or obscure the $\ln(v_d/v_u)$ signals over time. The mean $\ln(v_d/v_u)$ 60–100 s following the release of the heat pulse was used to calculate V_s (Fig. 4).

Thermal diffusivities, κ, were $(2.37 \pm 0.02) \times 10^{-3}$ and $(2.54 \pm 0.02) \times 10^{-3}$ cm^2 s^{-1} for *C. korshinskii* and *S. psammophila*, respectively. Heat-pulse velocity, V_h, was linearly correlated with V_s from gravimetric measurements of flow (R^2 up to 0.96, and $P < 0.001$) through all cut-stem sections from the two species (Fig. 5). V_s from the gravimetric measurements was as high as 49.3 cm h^{-1} for *C. korshinskii* and 28.7 cm h^{-1} for *S. psammophila*, subject to stem hydraulic properties and the limited pressure head that could be imposed; the corresponding measured V_h from the EHR gauges was 16.3 and 14.4 cm h^{-1} for *C. korshinskii* and *S. psammophila*, respectively. The m_{sap} multiplier for linearly correlating V_s with V_h was 2.02 for the *C. korshinskii* stems but was 43.1% lower, 1.15, for the *S. psammophila* stems. The m_{stem} multiplier was 0.78 for *C. korshinskii* and slightly lower, 0.67, for *S. psammophila*; the difference was due to significant differences in both stem bulk density and water content between the two species. m_{bark} was accordingly 2.59 for *C. korshinskii* but was 34.4% lower, 1.70, for *S. psammophila*. A higher m_{bark} indicates a larger attenuation in gauge output signals due to the effects of the non-hydroactive bark. Bark thickness was 0.8–1.04 mm for the *C. korshinskii* stems with diameters of 4.08–13.44 mm but was 0.42–0.72 mm for the *S. psammophila* stems with diameters of 5.81–15.6 mm. A thicker bark would decrease the exchange of heat from hydroactive tissues to the temperature sensors of the EHR gauge, which would lead to a larger m_{bark} for *C. korshinskii*; a dense stratum corneum on the surface of its bark would also impede heat transport.

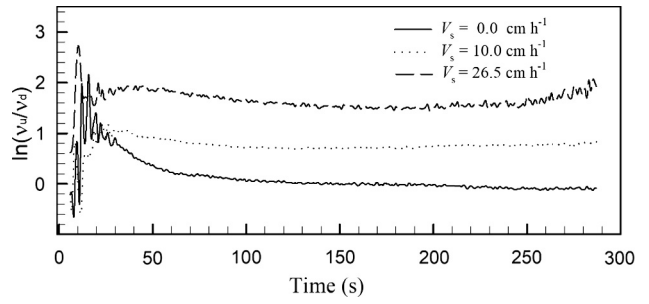

Fig. 4. Natural logarithm of the ratio of temperature rise ratio, $\ln(v_d/v_u)$, over time, estimated at various sap-flux densities (V_s, cm h^{-1}).

3.2. Sap-flow measurement in the field tests

V_s was measured on the *C. korshinskii* stems in the field using both the EHR and SHB gauges (Fig. 6a and b) over 26 days, and ET_0 was simultaneously estimated (Fig. 6c). Zero-flow conditions, used to correct EHR gauge misalignment, was acquired by removing all leaves from the stem canopy at the end of the field test, which eliminated the force driving canopy transpiration. Corrected x_d for the gauge misalignment correction was 0.96, 0.98 and 1.03 cm when x_u was assumed to be correctly spaced at 1.0 cm for the three gauges from Eq. (3). An alternative when such a destructive practice is not permitted is to capture the dynamics of $\ln(v_d/v_u)$ during the entire observation period and to empirically select the moments mostly indicating a zero-flow condition to correct for gauge misalignment.

Hourly V_s from the EHR gauges ranged between zero and 28.5 cm h^{-1} and usually had similar trends with ET_0, both within a day and over days. Hourly V_s fluctuated slightly more at high sap-flux densities at midday but was more stable and reliable at night. The EHR gauges captured the diurnal dynamics of V_s, especially at Days 4–6 when ET_0 decreased much more than other days, and the dynamics agreed well with the overall trends in ET_0. In contrast, V_s from the SHB gauges usually remained at zero between dusk and dawn and then sharply increased, which poorly represented the actual dynamics of sap flow, particularly at low densities.

The shallow soil profiles of this field had been recharged with ample rainwater in late spring and summer, so *C. korshinskii* did not suffer from drought stress during the field tests (Fan et al., 2016), and ET_0 was likely proportional to canopy transpiration. The linear regression analysis indicated that hourly V_s from the EHR gauges was significantly linearly correlated with ET_0 ($R^2 = 0.69$, $P < 0.001$; Fig. 7), and the datapoints were distributed relatively uniformly along the regression line for the full range of sap-flux densities (28.5 cm h^{-1} in this field test). Hourly V_s from the SHB gauges, however, was linearly correlated more weakly with ET_0 ($R^2 = 0.57$, $P < 0.001$) than from EHR gauges. When V_s from EHR gauges < 2 cm h^{-1}, the SHB gauges usually failed to give rational results.

4. Discussion

We introduced a new design of an EHR gauge better adapted to thin stems up to 15 mm in diameter than the previous design by Clearwater et al. (2009) dedicated to thinner plant organs and stems with diameters of 2 to 5 mm. The spacings between the heater and the bilateral temperature sensors was increased in this new design to 10.0 mm. The farther a temperature sensor is from the heat source, however, the less sensitive it will be to heat released by the heater (Burgess et al., 2001). The power of the heater was thus increased to prevent weak temperature signals at the larger spacings. The maximum recorded temperature rises were consequently within 0.2–0.6 and 0.6–1.6 °C at the upstream and downstream sensors, respectively, and temperature rises within these ranges could be appropriately measured under current thermometric resolution. The heater had a maximum temperature rise of 18 °C, and thermal injury indicated by darkening was observed at the contact

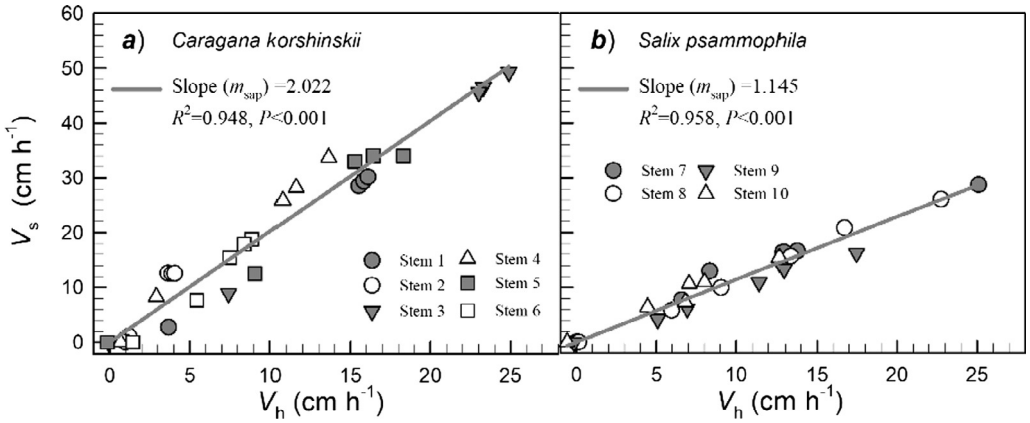

Fig. 5. Linear regression analysis between gravimetrically estimated sap-flux density (V_s, cm h^{-1}) and measured heat-pulse velocity (V_h, cm h^{-1}) from the EHR gauges on cut-stem sections of *Caragana korshinskii* (a) and *Salix psammophila* (b). The m_{sap} multiplier is defined in Eq. (8).

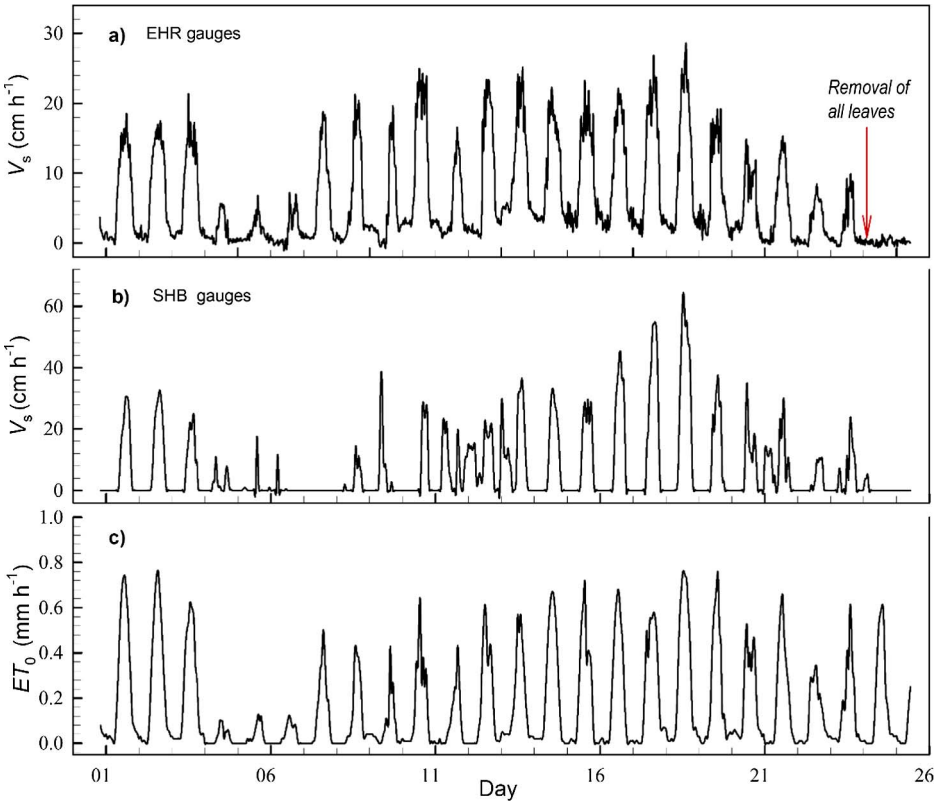

Fig. 6. Sap-flux density (V_s, cm h^{-1}) determined by the external heat-ratio (EHR) (a) and stem heat-balance (SHB) (b) gauges, and the reference evapotranspiration (ET_0, mm h^{-1}; c). All canopy leaves of the stems were removed on Day 25 to eliminate canopy transpiration and stop the flow of sap.

surface of the stem in the long-term field tests. This surface thermal injury, however, likely affected neither the deep bark tissues nor the status of stem growth, even in the thinnest stems we tested, and thicker stems generally have higher thermal tolerance permitting such heating.

The calculation of thermal diffusivity, κ, also relied on the gauge spacings. We derived κ by substituting the default gauge spacings, with means of 2.37×10^{-3} and 2.54×10^{-3} cm^2 s^{-1} for *C. korshinskii* and *S. psammophila*, respectively. Overestimating κ was likely, because it seldom exceeded 2.0×10^{-3} cm^2 s^{-1} over other studies using miniature EHR gauges, which contributed to the geometry of our heater. Large circular heaters introduce heat both above and below the center of the heater, so the heat will arrive at upstream and downstream locations faster or slower than the time needed to reach the maximum temperature rise, so κ is consequently overestimated. Supposing rates of κ, approaching to 1.6×10^{-3} cm^2 s^{-1} from Skelton et al. (2013) using gauges with very narrow heater, were more reliable and there had similar effective rates of κ in this studies, then effective gauge spacings were approximately 8 mm in our new configuration. The discrepancy associated with gauge configuration, however, has few impacts on measurements of sap flow, because its effects can be incorporated into the calibration coefficient, m_{sap}.

The stem bark affected the EHR measurements by interfering with the exchange of heat between the gauge heater, thermometric elements and internal xylem. The extent of these effects varied with bark thickness, heat-conducting property and contact firmness between the bark and gauge (Edwards et al., 1997). Bark thickness and stem structure differed greatly between the two species. m_{bark} was 2.59 and 1.70 for *C. korshinskii* and *S. psammophila*, respectively. *C. korshinskii* bark was significantly thicker and covered a hard, dense stratum corneum that was more resistant to the exchange of heat. EHR techniques will thus be

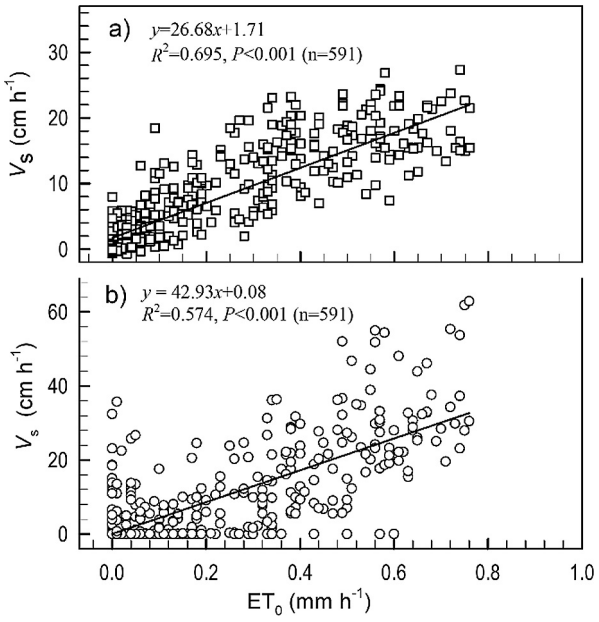

Fig. 7. Linear regression analysis between hourly sap-flux densities (V_s, cm h^{-1}) from the external heat-ratio (a) and stem heat-balance (b) gauges and reference evapotranspiration (ET_0, mm h^{-1}) in the *Caragana korshinskii* field.

inadequate for accurately measuring sap flow in stems with very thick bark and will require further assessment. Clearwater et al. (2009) reported that m_{bark} was ~1 after the removal of bark tissues, but such a severe tissue destruction should not be considered in practical applications.

The effects of stem properties and bark tissues do not need to be quantified in practice. Only one coefficient, m_{sap}, needs to be quantified in tests of gravimetric calibration to linearly convert the measured V_h into corrected V_s, to incorporate the effects of stem properties and bark tissues and to determine gauge configuration. m_{sap} has been reported for various plant species and functional organs and ranges in current and early studies, ranging from 1.7 to 7.8 (Clearwater et al., 2009; Skelton et al., 2013; Roddy and Dawson, 2012). Our EHR gauge requires separate calibration for specific gauge configurations before field application, in addition to careful empirical calibration based on species and type of functional plant organ. The newly designed external gauge can accurately estimate V_s in thin stems with diameters up to 15 mm and absolute densities < 50 cm h^{-1}, which covers most natural flux-density ranges. This study did not test stems with diameters > 15 mm, but stem diameter is not likely the key factor restricting the application of EHR methods in larger stems. EHR methods detect single-point sap flow, and non-uniform and radial variation of V_s distribution in stem cross sections would add variation in the representation of whole-stem V_s (Rungwattana and Hietz 2017). Our EHR gauge requires mounting on smooth stem sections away from knots, and cut-stem calibration tests should be performed at the end of an experiment using mounted gauges and cut sections from intact stems if the situation permits to minimize errors in changes in the status of the gauge mount.

Acknowledgements

The authors would give thanks to the support from the Projects of National Natural Science Foundation of China (NSFC 41571130082, 41571224). We would also thank Dr. Chenhui Li for assistance in our field work, and the editors and the anonymous reviews for their pertinent and valuable suggestions.

References

Baker, J.M., van Bavel, C.H.M., 1987. Measurement of mass flow of water in the stems of herbaceous plants. Plant Cell Environ. 10 (9), 777–782. http://dx.doi.org/10.1111/1365-3040.ep11604765.
Barrett, D.J., et al., 1995. Evaluation of the heat pulse velocity technique for measurement of sap flow in rain-forest and eucalypt forest species of south-eastern Australia. Plant Cell Environ. 18 (4), 463–469. http://dx.doi.org/10.1111/j.1365-3040.1995.tb00381.x.
Burgess, S.S., et al., 2001. An improved heat pulse method to measure low and reverse rates of sap flow in woody plants. Tree Physiol. 21 (9), 589–598. http://dx.doi.org/10.1093/treephys/21.9.589.
Burgess, S.S.O., et al., 1998. The redistribution of soil water by tree root systems. Oecologia 115 (3), 306–311. http://dx.doi.org/10.1007/s004420050521.
Clearwater, M.J., et al., 2009. An external heat pulse method for measurement of sap flow through fruit pedicels, leaf petioles and other small-diameter stems. Plant Cell Environ. 32 (12), 1652–1663. http://dx.doi.org/10.1111/j.1365-3040.2009.02026.x.
Cohen, Y., et al., 1981. Improvement of the heat pulse method for determining sap flow in trees. Plant Cell Environ. 4 (5), 391–397. http://dx.doi.org/10.1111/j.1365-3040.1981.tb02117.x.
David, T.S., et al., 2013. Root functioning, tree water use and hydraulic redistribution in Quercus suber trees: a modeling approach based on root sap flow. For. Ecol. Manage. 307, 136–146. http://dx.doi.org/10.1016/j.foreco.2013.07.012.
Dynamax Inc., 2005. Dynagage manual. < http://dynamax.com/images/uploads/papers/Dynagage_Manual.pdf > (access: 10 March, 2018).
Eastham, J., Gray, S.A., 1998. A preliminary evaluation of the suitability of sap flow sensors for use in scheduling vineyard irrigation. Am. J. Enol. Viticult. 49 (2), 171–176 http://www.ajevonline.org/content/49/2/171 (access: 10 March, 2018).
Edwards, W.R.N., et al., 1997. A unified nomenclature for sap flow measurements. Tree Physiol. 17 (1), 65–67. http://dx.doi.org/10.1093/treephys/17.1.65.
Fan, J., et al., 2016. Soil water depletion and recharge under different land cover in China's Loess Plateau. Ecohydrology. 9 (3), 396–406. http://dx.doi.org/10.1002/eco.1642.
Fernandez, J.E., et al., 2011. Combining sap flow and trunk diameter measurements to assess water needs in mature olive orchards. Environ. Exp. Bot. 72 (2), 330–338. http://dx.doi.org/10.1016/j.envexpbot.2011.04.004.
Green, S., et al., 2009. A re-analysis of heat pulse theory across a wide range of sap flows. In: 7th International Workshop on Sap Flow, Seville, Spain, 21-24 October 2008. International Society for Horticultural Science (ISHS), pp. 95–104 http://doi.org/10.17660/ActaHortic.2009.846.8.
Grime, V.L., Sinclair, F.L., 1999. Sources of error in stem heat balance sap flow measurements. Agr. Forest Meteoro. 94 (2), 103–121. http://dx.doi.org/10.1016/S0168-1923(99)00011-8.
Hernandez-Santana, V., et al., 2016. The dynamics of radial sap flux density reflects changes in stomatal conductance in response to soil and air water deficit. Agr. Forest Meteoro. 218–219, 92–101. http://dx.doi.org/10.1016/j.agrformet.2015.11.013.
Lu, P., et al., 2004. Granier's thermal dissipation probe (TDP) method for measuring sap flow in trees: theory and practice. Acta Botanica Sinica-English Edition 46 (6), 631–646.
Marshall, D.C., 1958. Measurement of sap flow in conifers by heat transport. Plant Physiol. 33 (6), 385–396. <http://www.jstor.org/stable/4259366>.
Nadezhdina, N., et al., 2015. Water uptake and hydraulic redistribution under a seasonal climate: long-term study in a rainfed olive orchard. Ecohydrology 8 (3), 387–397. http://dx.doi.org/10.1002/eco.1545.
Nakano, S., et al., 2015. Evaluation of the effects of increasing temperature on the transpiration rate and canopy conductance of soybean by using the sap flow method. J. Agric. Meteorol. 71 (2), 98–105. http://dx.doi.org/10.2480/agrmet.D-14-00046.
Roddy, A.B., Dawson T.E., 2012. Determining the water dynamics of flowering using miniature sap flow sensors. In: ISHS Acta Horticulturae 951: VIII International Symposium on Sap Flow. pp. 47–53. http://doi.org/10.17660/ActaHortic.2012.951.4.
Rosner, S., et al., 2018. Hydraulic and mechanical dysfunction of Norway spruce sapwood due to extreme summer drought in Scandinavia. For. Ecol. Manage. 409 (1), 527–540. http://dx.doi.org/10.1016/j.foreco.2017.11.051.
Rungwattana, K., Hietz, P., 2017. Radial variation of wood functional traits reflect size-related adaptations of tree mechanics and hydraulics. Funct. Ecol. 32 (2), 260–272. http://dx.doi.org/10.1111/1365-2435.12970.
Sakuratani, T., 1981. A heat balance method for measuring water flux in the stem of intact plants. J. Agric. Met. 37 (1), 9–17. http://dx.doi.org/10.2480/agrmet.37.9.
Sakuratani, T., 1984. Improvement of the probe for measuring water flow rate in intact plants with the stem heat balance method. J. Agric. Met. 40 (3), 273–277. http://dx.doi.org/10.2480/agrmet.40.273.
Skelton, R.P., et al., 2013. External heat-pulse method allows comparative sapflow measurements in diverse functional types in a Mediterranean-type shrubland in South Africa. Funct. Plant Biol. 40 (10), 1076–1087. http://dx.doi.org/10.1071/FP12379.
Smith, D.M., Allen, S.J., 1996. Measurement of sap flow in plant stems. J. Exp. Bot. 47 (12), 1833–1844. http://dx.doi.org/10.1093/jxb/47.12.1833.
Steppe, K., et al., 2015. Sap flow as a key trait in the understanding of plant hydraulic functioning. Tree Physiol. 35 (4), 341–345. http://dx.doi.org/10.1093/treephys/tpv033.
Trcala, M., Cermak, J., 2016. A new heat balance equation for sap flow calculation during continuous linear heating in tree sapwood. Appl. Therm. Eng. 102, 532–538. http://dx.doi.org/10.1016/j.applthermaleng.2016.03.092.
Vandegehuchte, M., et al., 2014. Influence of stem temperature changes on heat pulse sap flux density measurements. Tree Physiol. 35 (4), 346–353. http://dx.doi.org/10.1093/treephys/tpu068.
Walter I.A., et al., 2000. ASCE's standardized reference evapotranspiration equation. In: Watershed management and operations management 2000, pp. 1–11. https://ascelibrary.org/doi/abs/10.1061/40499%282000%29126.